

Signatures of Statistical Decay

D. Horn^a, G.C. Ball^a, D. R. Bowman^a, A. Galindo-Uribarri^a,
E. Hagberg^a, R. Laforest^{b *}, J. Pouliot^{b †}, and R. B. Walker^a

^a*AECL, Chalk River Laboratories, Chalk River, Ontario, K0J 1P0, Canada*

^b*Laboratoire de Physique Nucléaire, Université Laval, Ste-Foy, Québec, G1K 7P4,
Canada*

ABSTRACT

The partition of decay energy between the kinetic energy of reaction products and their Q-value of formation is obtained in a statistical derivation appropriate to highly excited nuclei, and is shown to be in a constant ratio. We measure the kinetic energy fraction, $R = \Sigma E_{kin} / (\Sigma E_{kin} + \Sigma Q_0)$, over a wide range of excitation energy for well-defined systems formed in the $^{35}\text{Cl} + ^{12}\text{C}$ reaction at 35A MeV. Relationships between excitation energy, charged-particle multiplicity, and intermediate-mass-fragment multiplicity, observed in this work and in recent experiments by a number of other groups, follow from the derivation of the average kinetic energies and Q-values.

1. Introduction

A number of scaling phenomena and correlations between observables have recently been discovered in the deexcitation of highly excited nuclei. These include:

- the correlation of N_{IMF} , the number of intermediate-mass fragments, with N_c , the total number of charged products,¹
- the correlation of N_{IMF} with Z_{bound} , the total amount of charge contained in fragments heavier than hydrogen,²
- the approximate proportionality of N_{IMF} to E_t , the measured transverse energy,³
- the linear relationship between N_c and T , the nuclear temperature,⁴ and
- the scaling of IMF multiplicity yield ratios with $\frac{1}{\sqrt{E_t}}$.^{5,6}

Each of these observations has been taken as indicative of statistical decay. We here introduce a schematic derivation for the partitioning of the decay energy between the kinetic and the mass-excess degrees of freedom. Because of its relatively small width at moderate multiplicities, the ratio of the kinetic energy of the products to the total available decay energy is proposed as an event-by-event signature for statistical

*Present address: Laboratoire de Physique Corpusculaire, ISMRA et Université de Caen, Blvd. du Maréchal Juin, F-14050 Caen, France.

†Present address: Hôtel-Dieu de Québec, Département de Radio-Oncologie, Québec, Canada.

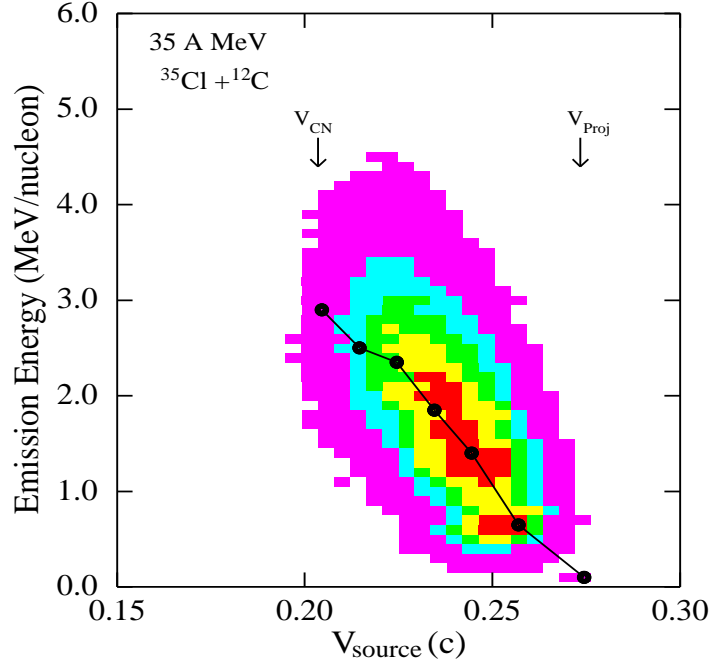


Fig. 1: Emission energy ($E_{kin} + Q_0$) per nucleon in the moving frame plotted as a function of the velocity of the center of mass of the detected fragments for 35A MeV $^{35}\text{Cl} + ^{12}\text{C}$. Points represent a massive-transfer simulation, filtered by the experimental acceptance; arrows indicate the velocities of the projectile and of the projectile-target center of mass.

decay. Further consequences of the derivation include the dependence of the mean multiplicities, $\langle N_c \rangle$ and $\langle N_{IMF} \rangle$, on excitation energy and the prediction of multiplicity yield ratios. The derived quantities are confronted with our experimental results for the decay of light nuclear systems with measured velocities, sizes, and excitation energies.

2. Derivation of Statistical Observables

The probability of emitting a particle with kinetic energy, E_{kin} , from a state of excitation energy, E , is

$$P(E, E_{kin}, Q_0) \propto E_{kin} \sigma_{inv}(E_{kin}) \frac{\rho_f(E - E_{kin} - Q_0)}{\rho_i(E)}, \quad (1)$$

where ρ_f and ρ_i are the final- and initial-state level densities and $\sigma_{inv}(E_{kin})$ is the cross section for the inverse reaction. The mean kinetic energy may be derived by integrating E_{kin} with the probability distribution of equation (1):

$$\langle E_{kin} \rangle = \frac{\int_0^{E-Q_0} E_{kin} P(E_{kin}) dE_{kin}}{\int_0^{E-Q_0} P(E_{kin}) dE_{kin}}. \quad (2)$$

In the limit of high excitation energy and negligible emission barriers, this gives the traditional⁷ results for the mean kinetic energy,

$$\langle E_{kin} \rangle = 2\sqrt{E/a} = 2T, \quad (3)$$

and its variance,

$$\sigma_{E_{kin}}^2 = 2E/a = 2T^2, \quad (4)$$

where a is the nuclear level-density parameter. These results are appropriate for neutron emission and for charged-particle emission from light systems, where Coulomb barriers are very low. The many exit channels accessible to states of high excitation energy permit one to approximate the density of available ground-state Q-values as a continuous function, $f(Q_0)$. A similar integral may then be performed for Q_0 , also giving a proportionality to $\sqrt{E/a}$, with the proportionality constant depending on $f(Q_0)$. Thus,

$$\langle Q_0 \rangle = 2\sqrt{E/a} = 2T \quad (5)$$

if the density of available exit channels is a linear function of Q_0 . For systems in the mass range studied experimentally here, this is a reasonable approximation. Whatever the proportionality factor, the kinetic energy fraction,

$$R = \frac{\Sigma E_{kin}}{(\Sigma E_{kin} + \Sigma Q_0)}, \quad (6)$$

should then be a constant, independent of excitation energy, with the specific case of $\langle Q_0 \rangle = 2T$, giving $\langle R \rangle = 0.50$.

For statistical processes, the observed width depends on the number of samplings of the parent distribution. In our case the number of samplings is the number, N , of detected charged particles. For $\langle R \rangle = 0.50$, that width is

$$\sigma_R = \frac{1}{4\sqrt{2N}}. \quad (7)$$

We now examine the relative *rates* for barrier-dominated and barrier-independent emission. If the probability per unit time for emitting n particles is approximately proportional to $\exp(-n \langle \Delta E \rangle / T)$, where $\langle \Delta E \rangle$ is the average deexcitation energy per particle emitted, then the particle emission *rate* is

$$\langle n \rangle = \frac{\int dn n \exp(-n\Delta E/T)}{\int dn \exp(-n\Delta E/T)} \propto \frac{T}{\Delta E}. \quad (8)$$

For light-ion emission from a light, highly excited nucleus, we neglect the Coulomb barrier and obtain

$$\langle \Delta E \rangle = \langle E_{kin} \rangle + \langle Q_0 \rangle = 4T. \quad (9)$$

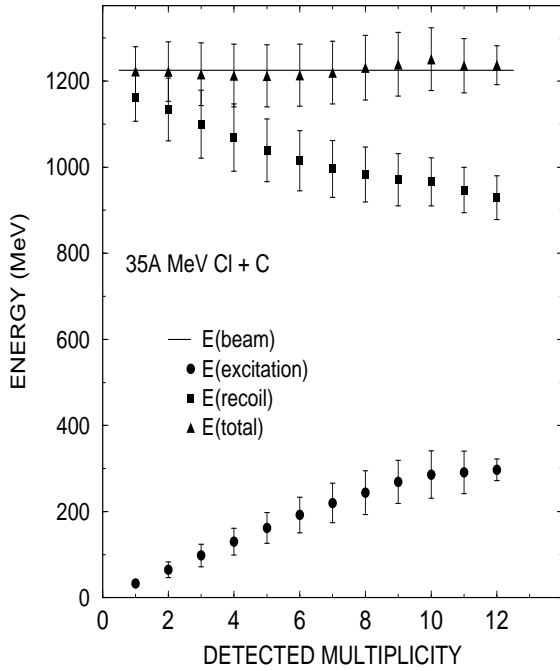


Fig. 2: Energy sums and distribution widths (bars) for 35A MeV $^{35}\text{Cl}+^{12}\text{C}$ as a function of the number of detected charged particles. The solid line indicates the beam energy.

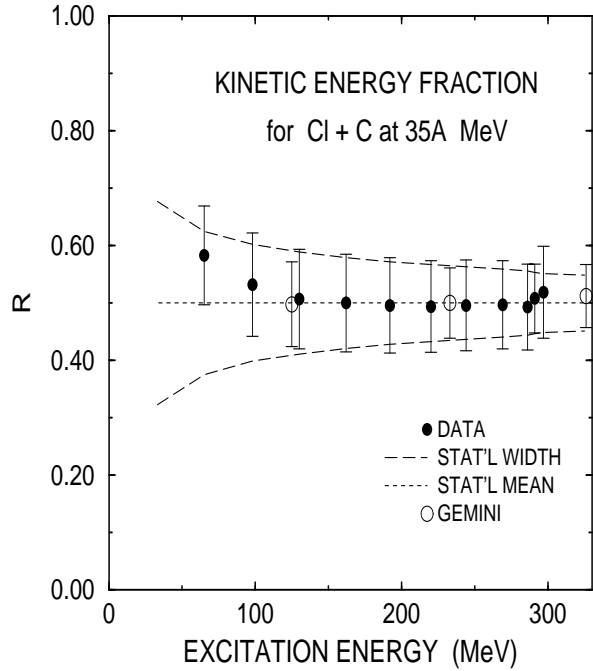


Fig. 3: Centroids and widths of kinetic energy fraction, R , for $^{35}\text{Cl} + ^{12}\text{C}$ at 35A MeV. Data for multiplicities 2 to 12 are plotted.

However, for emission of heavier fragments, barrier effects may dominate, so that $\langle \Delta E \rangle \approx B$. A fixed or generic value of B , previously demonstrated⁵ to be appropriate for IMF emission, would imply the rates for the two processes to be in the ratio,

$$\frac{\langle n_{IMF} \rangle}{\langle n \rangle} \propto \frac{T/B}{T/4T} \propto T. \quad (10)$$

If the average deexcitation per particle is $\langle \Delta E \rangle = 4T$, the mean number of particles emitted would be $\langle N \rangle = E/4T$, giving

$$N \propto \sqrt{E}, \quad (11)$$

and variance,

$$\sigma_N^2 = N/4. \quad (12)$$

From the ratio of rates,

$$N_{IMF} \propto E. \quad (13)$$

If the proportionality of transverse energy to excitation energy is assumed, then equations (11) and (13) consolidate the first four points of the introduction.

3. Experimental Determination of Source Properties

A systematic comparison of the derived quantities with experiment requires the event-by-event determination of the size, velocity and excitation energy of the decaying system. One type of reaction which lends itself to the isolation and measurement of an excited source is the massive transfer mechanism⁸. A beam of 35A MeV ³⁵Cl ions, provided by Chalk River's TASCC facility, collided with a 2-mg/cm² carbon target, producing a variety of reaction products. The kinematics of the reaction served to focus the reaction products into the 6° to 25° angular range of our detector array, a close-packed assembly of 40 phoswich counters⁹. All ions were identified by atomic number and isotopic distributions were measured with a set of high-resolution Si/CsI detector telescopes.¹⁰ Our selection of massive transfer events was facilitated by the thresholds and limited angular acceptance of the array, which reduced our sensitivity to target-like “spectator” matter.

To ensure that no major component of an event went undetected, we analyzed only events in which at least 15 units of charge were identified. The velocity of the center of mass of all detected ions was computed, and the kinetic energy of each product was calculated within the moving frame. Based on the average mass excess deduced from the isotope distributions for each detected ion, ΣQ_0 was added to ΣE_{kin} for each event, and the resulting deexcitation energy per detected nucleon was plotted as a function of source velocity. Fig. 1 shows the relationship between emission energy per nucleon and source velocity, starting at projectile-like values of source velocity and zero emission energy in the lower right portion of the figure, and extending to compound-nucleus velocity and large emission energy in the upper left. The entire range of massive transfer phenomena, as previously observed at lower energies¹¹, is evident in the figure. The points superimposed on the figure represent centroids of the distributions in energy and velocity for the simulated massive transfer of zero to twelve nucleons from the carbon target to the heavier projectile. Decay of the excited system is simulated¹² by a Monte Carlo event generator and filtered by the experimental acceptance. Quantitative agreement with the data has been demonstrated¹³ for simultaneous projection of the same set of calculated results on both the energy and velocity axes.

A massive transfer reaction has the useful feature that the mass of the recoiling system may be deduced from its velocity, allowing a model-dependent estimate of total excitation energy. The validity of this estimate can then be tested by the consistency check demonstrated in Fig. 2, where the excitation energy, recoil energy, and deduced total energy are plotted as a function of the number of detected charged particles. Here, the multiplicity-dependence of the momentum transfer and energy deposition is evident. Significantly, the energy sums yield the initial projectile energy, indicating that the efficiency corrections have been properly applied. The behavior of any unobserved component must then be consistent with that of the detected fragments.

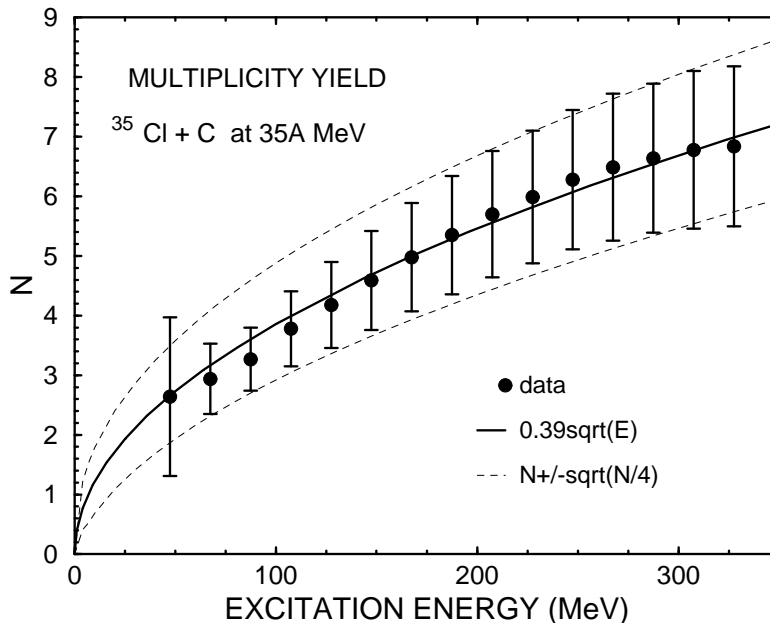


Fig. 4: Centroids and widths of multiplicity distributions for $^{35}\text{Cl} + ^{12}\text{C}$ at 35A MeV, plotted as a function of reconstructed excitation energy. The proportionality constant for the solid line, $k = 0.39$, was chosen to fit the data.

4. Comparison of Derived and Measured Statistical Observables

Fig. 3 shows the kinetic energy fraction, R , plotted as a function of excitation energy for events in which two to twelve charged products were detected. The excitation energy attributed to each point is the mean for a given multiplicity. Filled circles are the centroids of the R distributions, with bars indicating the distribution widths, σ_R . The $\langle R \rangle = 0.50$ value and associated widths from equation (7) are indicated by the dashed curves. To investigate the effects of a more comprehensive statistical treatment, a calculation was performed with the code, GEMINI¹⁴, with average gamma-ray emission energies obtained from a modified version of PACE¹⁵, and the results for three excitation energies plotted as open circles. The data are obviously in good agreement with both the schematic calculation and the statistical code results, though some bias due to detector acceptance may be apparent at the lowest multiplicities. The statistical nature of the decay is reflected in the R distributions over the range of excitation energies from 2 to nearly 7 MeV per nucleon. The narrowness of the distribution supports the prediction of equation (7) and indicates that, even for relatively low multiplicities, R may be useful as an event-by-event indicator of statistical decay. Indeed, the technique has recently been applied to a series of projectile fragmentation experiments¹⁶, giving $\langle R \rangle$ values from 0.50 to 0.57.

The mean number of charged fragments emitted should, according to equation (11), be proportional to the square root of the excitation energy. Fig. 4 shows the centroids and widths of the measured multiplicity distributions as a function of

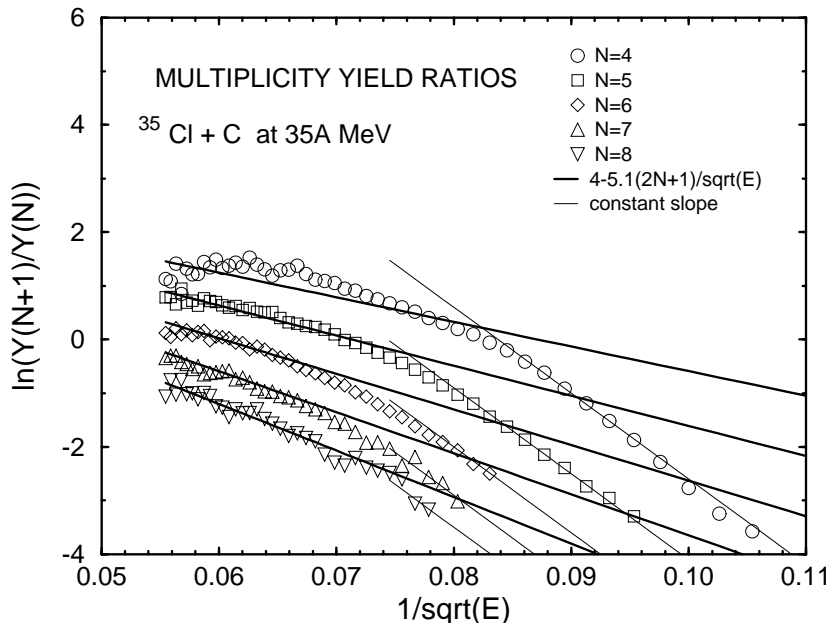


Fig. 5: Natural logarithm of multiplicity yield ratios for $^{35}\text{Cl} + ^{12}\text{C}$ at 35A MeV, plotted as a function of $E^{-1/2}$. Heavy lines represent ratios based on “barrier-independent” calculations of N and σ ; light lines represent constant slope.

excitation energy. The solid line represents a square-root proportionality, and the widths determined by equation (12) are indicated by the dashed lines. The centroids and widths predicted by our schematic statistical derivation are in good agreement with experiment for the higher excitation energies, but at lower energies, where the Coulomb barrier might impose upper limits on the number of charged particles, the experimental widths are narrower.

Moretto *et al.*⁵ have demonstrated that for IMF emission, which may be dominated by barrier effects, the natural logarithm of the multiplicity yield ratio is a linear function of $E^{-1/2}$. We plot this ratio for emission of *all* ions in Fig.5. Note that the data do not, except at the lowest excitation energies, have the linear dependence upon $E^{-1/2}$ expected from the systematics of ref. 5. Based on the behavior of the widths in Fig. 4, it would instead be reasonable to expect agreement at higher excitations with multiplicity yield ratios predicted for barrier-independent emission. In this case, the assumption of gaussian multiplicity distributions gives

$$\ln\left(\frac{Y(N+1)}{Y(N)}\right) = 4 - \frac{2(2N+1)}{k\sqrt{E}}, \quad (14)$$

where k is the proportionality constant of equation (11). These “statistical” ratios, indicated by the heavy lines in Fig. 5, do, in fact, approximate the data at high excitation energies. For lower excitation energies, the constant slopes of the barrier-dominated systematics may be more appropriate.

5. Conclusions

- A schematic calculation showed, for $E \gg B$, that the partition of decay energy between kinetic energy of emission and Q_0 should be in a constant ratio for statistical decay.
- The kinetic energy fraction, $R = \Sigma E_{kin}/(\Sigma E_{kin} + \Sigma Q_0)$, and its width were measured for a well-determined reaction mechanism.
- The predicted mean and distribution width for R were observed in the data and reproduced in calculations with a well-known statistical decay code.
- At sub-vaporization excitation energies, emission at the barrier has a different energy dependence than emission well above the barrier.
- The relationship between the two processes is exemplified by many of the correlations observed between charged-particle production, IMF production, and excitation energy.

6. References

- [1] D.R. Bowman *et al.*, Phys. Rev. **C46** (1992) 1834.
- [2] J. Hubele *et al.*, Z. Phys **A340** (1991) 263.
- [3] L. Phair, private communication.
- [4] N. Porile, Proc. XI Winter Workshop on Nuclear Dynamics, Key West, Florida, 1995 Feb 11-17.
- [5] L.G. Moretto, D.N. Delis, and G.J. Wozniak, Phys. Rev. Lett. **71** (1993) 3935.
- [6] L.G. Moretto *et al.*, Phys. Rev. Lett. **74** (1995) 1530.
- [7] P. Morrison in *Experimental Nuclear Physics, Vol. II*, ed. E. Segré (John Wiley and Sons, New York, 1953), p.173.
- [8] P.J. Siemens *et al.*, Phys. Lett. **36B** (1971) 24.
- [9] C. Pruneau *et al.*, Nucl. Inst. and Meth. in Phys. Res. **A297** (1990) 404.
- [10] D. Horn *et al.*, Nucl. Inst. and Meth. in Phys. Res. **A320** (1992) 273.
- [11] N. Colonna *et al.*, Phys. Rev. Lett. **62** (1989) 1833.
- [12] D. Horn *et al.*, PR-TASCC-4: 3.1.7; AECL-10545.
- [13] D. Horn *et al.*, Proc. Int. Workshop on Heavy-Ion Fusion, Padova, Italy, 1994 May 24-27, editors A.M. Stefanini *et al.* (World Scientific, 1994) 208.
- [14] GEMINI code: R.J. Charity *et al.*, Nucl. Phys. **A483**(1988)371.
- [15] PACE2 code: A. Gavron, Phys. Rev. **C21** (1980) 230, modified by J.R. Beene.
- [16] R. Roy *et al.*, to be published in Proc XXXIII International Winter Meeting on Nuclear Physics, Bormio, Italy, 1995 Jan 23-28.